International Journal of Sciences

Research Article Volume 3 - December 2014 (12)

MTCBP-1 Protein Expression is Enhanced in Fat Overloaded HepG2

Masego Tsimako Johnstone[1,2], Paul Kroon[1], Peter Wilce[1]

[1]School of Chemistry and Molecular Sciences, University of Queeensland, Brisbane, St Lucia, Australia
[2]Department of Biological Sciences, Faculty of Science, University of Botswana, Gaborone, Botswana

ABSTRACT

Background: Macrovesicular steatosis, is characterised as excessive triglyceride accumulation in the liver which perpetuate cell injury through signalling cascades. Although there are several hypotheses that have been proposed in liver damage, it is unclear as to how the events occur as well identification of the key proteins that facilitate this event.

Aims: HepG2 *in vitro* fat cell model was used to investigate the relationship between cellular triglycerides and MTCBP-1 expression.

Methods: The cells were treated with linoleic acid conjugated to defatted BSA. There were two controls to the experiments, consisting of cells grown in 10% defatted BSA and normal growth medium. Triglycerides were analysed by a quantitative standard curve and nile red staining. Western blots were used for detection of MTCBP-1 in transfected and untransfected cells grown in LA-BSA and compared with control cells. The subcellular localisation of MTCBP-1 was also determined by immunofluorescence.

Results: Nile red staining of HepG2 showed presence of triglyceride mainly in the cytoplasm, with higher amounts of lipid droplets found in LA-BSA treated cells. The lipid treated cells contained a significantly increased amount of triglycerides ($\rho = 0.004$). Lipid overloaded HepG2 cells transfected with pSG5 plasmid encoding c-myc-MTCBP-1 contained much lower triglycerides when compared with the untransfected HepG2 cells. There was an increased expression of endogenous MTCBP-1 in lipid overloaded cells. MTCBP-1 is located in the cytoplasm and nucleus of the cell.

Conclusion: The increased expression of MTCBP-1 during triglyceride accumulation may suggest a relationship between the protein and triglyceride synthesis. It can further be explored as a potential target in therapeutics/diagnostics. The next step is to understand the interaction of MTCBP-1 with other proteins in triglyceride synthesis and packaging.

1 Introduction

The liver plays a vital role in homeostatis by storing sugars and metabolising them for fuel supply in peripheral organs. However, if there is a defect in the liver function as a consequence of hepatic steatosis, this may result in impaired usage of fatty acids in liver cells and increased lipid accumulation. This excessive triglycerides in a steatoticliver is considered a source of reactive oxygen species that mediate lipid peroxidation and perpetuate cell injury through signalling cascades proposed in the 2-hit hypothesis studies [4, 25].

Hepatic steatosis is a liver disorder that falls under the spectrum of non-alcoholic fatty liver disease (NAFLD). NAFLD is a common disease worldwide, particularly in the western countries, where it is associated with body weight and lifestyle (Susuki, A. 2005);owever, knowledge on the molecular mechanisms leading to steatosis and further disease advancement remains unclear, hence there are limited therapeutic strategies established for the diasease [1,12-17]. Currently there are on-going studies on Human NASH [2,3,12-17], NASH animal models [13, 14] and NASH *in vitro* models [4,14,18, 24] that aim to provide better understanding of the key players in steatosis leading to NASH/NAFLD [2,3].

We previously identified *MTCBP-1* gene from human NAFLD DNA microarrays (unpublished data). The protein encoded by the gene has been shown to play a role in cancer progression, by negatively regulating the multifunctional membrane type-1 metalloproteinase (MT1-MMP) which functions in promoting tumour growth, invasion and metastasis [5,8,9]. Thus, bound MTCBP-1 hinders cell migration and invasion [5, 7]. MTCBP-1 is a 19 kD

Masego Tsimako Johnstone (Correspondence)
masego.johnstone@mopipi.ub.bw
+

protein which belongs to the *Cupin* superfamily that consists of functionally diverse proteins with a conserved *β*-barrel fold [5,7,10]. The role of MTCBP-1 in steatosis and NASH pathogenesis however remains unknown.

Blast searches, reveal MTCBP-1 to be a highly conserved protein whose homologues exist between evolutionary distant species including: *Homo sapiens*, bacterial acid-reductone dioxygenase (ARD), *Saccharomyces cerevisiae* and rats (figure 1). MTCBP-1 shares a striking resemblance to *N*-terminus truncated human Sip-L which supports hepatitis C virus (HCV) replication in non-permissive cell line [11], however, little is known about the mechanism through which Sip-L supports HCV replication. In our study we utilised linoleic fatty acid (C18:2) conjugated to defatted bovine serum albumin (BSA) in cultures of human hepatoblastoma cells to mimic cellular steatosis and analyse the levels of cell triglycerides as well as the endogenous MTCBP-1 protein expression and over-expressed MTCBP-1.

2 Materials and Methods

2.1 Materials

The human hepatoblastoma cell line HepG2 was a donation from Professor Grant Ramm, Hepatology Department, Queensland Institute of Medical Research (QIMR). RPMI 1640 medium, foetal bovine serum (FBS) trypsin, penicillin/streptomycin and glutamate were purchased from GIBCO Australia. Bovine serum albumin (BSA), oleic acid-conjugated BSA (OA-BSA), linoleic acid-conjugated BSA (LA-BSA) and Nile Red was obtained from Sigma-Aldrich. Triglyceride standards and liquid stable reagent are products of Thermo Electron Corporation. Lipofectamine 2000 transfection reagent was purchased from Invitrogen. The peptide affinity purified polyclonal rabbit antibody against MTCBP-1 was produced in our lab. The plasmid encoding human MTCBP-1 cDNA was a donation by Professor Motoharu Seiki, Division of Cancer Research, Institute of Medical Science and University of Tokyo, Japan.

2.2 Production of peptide affinity purified polyclonal rabbit antibody

Antigenic peptide regions of MTCBP1 protein sequence were analysed using Preditop algorithm (Appendix 1). The peptides displaying the highest antigenicity were selected for peptide synthesis by standardised solid-phase FMOC chemistry that utilise HBTU amino acid coupling group [33]. Synthesis was performed on commercially available Rink-Amide resin protected at the alpha-amino group with the labile FMOC protecting group and protected orthogonally with a typical amino acid specific protecting group. The peptides were checked by MALDI-TOF mass spectrometry after coupling of every fourth amino acid to confirm intermediate masses and final masses were checked after the last amino acid was added (Appendix 2) Completed peptides were simultaneously cleaved from the resin and purified on reverse phase. Following that, the peptide was conjugated to ovalbumin carrier protein for immunisation of New Zealand white rabbits. The antibody titres were analysed using ELISA (Appendix 3).

2.3 Cell Culture

HepG2 cells were cultured in RPMI media supplemented with 10% foetal Bovine Serum (FBS), 2 mM glutamine, and 100U/mL of penicillin/streptomycin under humidified atmosphere of 95% air and 5% CO_2. Cell viability was checked by Trypan blue exclusion test.

2.4 Fatty acids overloading in hepatocytes

The cells were seeded at 2 x10^6 per well in a 6 well culture plate (with and without coverslips) and grown in an enriched medium of 0.5 mM LA-BSA to 40-60% confluency. A negative control experiment was also performed, consisting of 10% BSA in PBS. All experiments were performed in triplicates and cells were grown for a period of 24 hours.

2.5 Flouresent Lipid staining

Cells grown in lipid rich medium and control medium were washed twice with PBS and fixed with 4% formaldehyde for 20 minutes. The cells were incubated in 100 µg/mL nile red at room temperature for 6 min. Following that, the cells were washed twice in PBS, with gentle rocking and mounted onto a slide using DAKO fluorescent medium for viewing under fluorescent microscope.

2.6 Plasmid construction

MTCBP-1 cDNA was a donation by Professor Seiki [7]. The *MTCBP-1* construct was re-cloned into pSG5 mammalian expression vector using restriction sites *EcoRI* and *BglII*. Briefly, the 5'UTR of *MTCBP-1* construct was replaced with a c-myc tag by PCR cloning with primers 5'AGTC GAATTC CCACCATG GAGCAGAAACTCATCTCTGAAGAGGATCTG GTGCAGGCCTGGTATATG 3' (forward primer) and 5' AGTC AGATCT CTAGGCGGTCTGTGCCAGA 3' (reverse primer). The forward primer consisted of four randomly chosen nucleotides to enhance the cleavage efficiency, an *EcoRI* restriction site, a Kozak sequence which contains a start (Met) codon, a c-myc tag sequence (30 base pairs) and the gene specific sequence (18 base pairs). The reverse primer consisted of four extra nucleotides, *BglII* restriction site and a gene specific sequence which contains a stop codon. The PCR amplification was performed on a preheated thermal cycler under initial denaturation conditions of 94ºC for 1 min and 45 sec followed by

26 cycles of 45 sec at 94ºC and 1 min annealing at 90ºC. The amplicons (Figure 3) were analysed on 0.6% (g/v) agarose gel. The PCR product was excised from the gel using QIAGEN gel extraction kit, following the manufacturers' protocol and then sequenced.

2.7 Transfection of MTCBP-1 expression vector into HepG2 cells

Transient transfections with pSG5-cmyc-MTCBP-1 construct and control vector pSG5-cmyc-MTA were carried out using Lipofectamine 2000 transfection reagent. Transfections for western blot analyses were performed in 6 well plates in triplicates (2 x 10^6 cells per well) and the cells were grown to ~70% confluency prior to transfection. For immunocytochemistry, the cells were grown on coverslips in a 24 well plate (2 x 10^5 cells per well) for 24 hours. Lipid overloading of cells with LA-BSA was carried out 24 hrs prior to transfections and included two control experiments, one with 10% BSA and the other, a normal culture growth in medium free of fatty acids and BSA. For six well plate transfections, 2µg of DNA and 5µL of the transfection reagent were used per well. For transfection in a 24 well plate, 400ng of DNA and 1µL lipofectamine reagent were used. The DNA and lipofectamine were prepared in Opti-MEM® I reduced serum medium (GIBCO). All transfections were carried out in antibiotic free media for 48 hr, following the reagent manufacturers' protocol. The transfections were monitored with ONPG assay for beta-galactosidase activity and were repeated independently at least once for reproducibility.

2.8 Cell lysate preparation, triglyceride analysis and detection of MTCBP-1

The cells were washed twice with cold Ca^{2+}, Mg^{2+} free PBS to remove any traces of the media. Cells were then lysed using cold lysis buffer (100µL per well) containing 1% Triton X100, 150 mM NaCl, 10mM Tris Base pH 7.4, 1mM EDTA, 1mM EGTA pH 8.0, 0.2mM sodium orthovandate, 0.5% Igepal, protease cocktail inhibitor (1µL/mL). The cells lysate was then passed through a 25-Gauge needle (10 passages) to break open the cells and centrifuged for 30 minutes at 10 000 x *g*. The supernatant collected was used for triglycerides (TG) and western blot assays A triglyceride standard curve was constructed in a range of 50 - 2000µg/mL of the triglyceride reagent (ThermoTrace, Australia), following the manufacturers protocol. A protein standard curve within the range 0.1 – 1.0 mg/mL was constructed from BSA using Bicinchoninic acid (Sigma-Aldrich, USA), following the manufacturers protocol. A 10µg of protein in lysate was separated on a 14% PAGE and transferred to a nitrocellulose membrane (Pall Corporation). The membrane was blocked for 2 hr with 3% fish gelatine and the protein was probed separately with peptide-affinity purified antibodies against MTCBP-1 and polyclonal c-myc antibody (Sigma) for detection of endogenous or expressed MTCBP-1. A fluorescent secondary antibody (anti-rabbit IgG conjugated with a flourophore) which absorbs at a wavelength of 680 nm was used for visualisation of the blot using an Odyssey Infrared Imaging System (*LI-COR* Biosciences).

2.9 Immunofluorescence staining

Lipid overloaded and transfected HepG2 grown in coverslips were washed three times in PBS and fixed with 4% paraformaldehyde in PBS. The cells were then permeabilised in 0.3% Triton X-100 in PBS for 10 minutes and blocked for one hour in 1% BSA, 0.3% Triton in PBS. The polyclonal anti-MTCBP-1 primary antibody was incubated in cells overnight while monoclonal anti-cmyc antibody (Sigma) was incubated for two hours. Following that, the cells were incubated with fluorescent secondary antibodies Alexa 488-conjugated goat anti-rabbit IgG (Molecular Probes) and Alexa 594-conjugated goat anti-mouse IgG (Molecular Probes) for visualisation of MTCBP-1 and c-myc tagged MTCBP-1, respectively. The cells mounted on slides using DAKO medium and visualised under Zeiss LSM 510 confocal laser microscope.

3 Results and discussion

3.1 Nile red fluorescent staining for triglycerides

HepG2 cells that were grown on coverslips in varying concentrations of LA-BSA in media were stained with nile red for determination of triglyceride incorporation in cells (Figure 2). The lipid overloaded cells had small and a few large round bodies distributed around the cytoplasm, mostly forming clusters. These round bodies are typically cytoplasmic fat droplets that are formed as a result of the uptake of fatty acid by the cells. The nuclei appeared mostly dark, although a few cells contained a scarce amount of the lipid droplets. The small discrete bodies seemed more prominent in cells treated with high concentrations of LA-BSA and were demonstrated in most cells. In contrast, the control cells which were grown in a medium containing 10% BSA showed only a few of the fat droplets, most of which were really small. HepG2 cells were still viable after addition of free fatty acid concentrations of up to 0.5mM; however, the addition of fats altered the cell morphology, as cells appeared more rounded in shape. The cytoplasmic inclusions stained with nile red are triglyceride accumulations and a large cluster of them, as demonstrated in lipid overloaded cells, resemble hepatic microvesicular steatosis.

3.2 Triglyceride and protein levels in lipid overloaded cell model

The cellular triglycerides incorporated in cells exposed to albumin-bound FFA were expressed as a ratio of triglyceride concentration to total protein

content. Figure 6 shows that HepG2 cells incubated with LA-BSA contained an elevated amount of triglycerides ($\rho = 0.004$) compared to triglycerides levels from control cells grown in media containing 10% BSA and normal culture medium free of BSA and fatty acids. An approximate 2-fold increase in triglyceride levels was obtained in LA-BSA treated cells when compared with triplicated control cells treated with BSA while a ~9-fold increase was obtained relative to untreated control cells.

Cellular triglycerides were also analysed from transfected HepG2 cells to determine if overexpressed protein affected the levels of triglycerides. HepG2 cells grown in a medium containing LA-BSA and transfected with pSG5 plasmid encoding c-myc-MTCBP-1 contained much lower triglyceride levels (4-fold less) when compared with the untransfected HepG2 cells. Furthermore, a one way ANOVA analysis of variance showed that there was no significant difference ($\rho = 0.067$) in cellular triglyceride levels from HepG2 cells that were overloaded with FFA and transfected with a plasmid encoding MTCBP-1 compared with triglycerides from the control cells. When HepG2 cells were transfected without any plasmid DNA, the triglyceride levels were found to be slightly higher in cells grown in a medium containing LA-BSA, although this increase was not statistically significant ($\rho=0.577$). Summarised in table 1 are the ratio of cellular triglycerides, fold-changes and p-values for HepG2 cells treated with LA-BSA.

Triglycerides are glycerides which are esterified with free fatty acids. Although fatty acids are essential biological components, their elevated concentrations have been linked to disorders such as obesity, atherosclerosis and diabetes. Thus, the physiological levels of fatty acids must be maintained within moderate levels. The transport of triglyceride through the body is vital in maintenance of physiological energy balance, thus incorporation of this lipid into large particles called lipoproteins, allows it to be delivered to a variety of tissues via the blood stream [26-28]. Very low density lipoprotein (VLDL) is the main transporter of endogenous TG and the production of this lipoprotein is regulated by hepatic synthesis of TG.

There are several mechanisms through which polyunsaturated fatty acids (PUFA) such as oleic and linoleic acids may promote triglyceride synthesis. The unsaturated fatty acids can serve as ligands for transcription factors peroxisome proliferator-activated receptor (PPAR). While there are 3 subtypes of PPARs, PPARα and PPARγ are the only subtypes that have been shown to play a role in catabolism and storage of fatty acids, respectively. PPARα and PPARγ are expressed in several tissues, such as the liver, colon, macrophages and the heart. Studies on rodents have revealed that animals treated with FA result in elevation of peroxisomes and induction of hepatic genes involved in β-oxidation of FA in peroxisomes, mitochondria and other cell compartments [20-22]. Fatty acids not destined for mitochondrial β-oxidation or peroxisomal oxidation may be esterified to triglycerides or other lipids.

Several studies have looked at the mechanisms by which newly synthesised triglycerides become incorporated into the core of VLDL [28-30]. Triglycerides exist as TG-enriched globules in the ER and combine with immature VLDL particle in the second step of the assembly. Triglycerides synthesised from FA that are destined for incorporation into VLDL are temporarily stored within the cell cytosol. Wu *et al.* (1996), has identified two different pools for triglyceride storage in HepG2 cells, namely: the cytosolic and microsomal pools. The majority of the newly synthesised TG enters the cytosolic pool which does not contribute to the VLDL assembly, while some enter the microsomal pool that contributes to most of the triglyceride present in newly synthesised VLDL.

3.3 Endogenous MTCBP-1 is increased in the fat cell model

HepG2 cells were grown in medium containing LA-BSA in an effort to determine MTCBP-1 protein expression pattern in fat overloaded cells, representative of steatosis. For comparison, controls consisting of HepG2 cells grown in medium containing BSA and normal culture medium with no added BSA were included. Protein expression in cell lysates from FFA treated HepG2 cells and control cells were determined relative to *β*-actin using the Odyssey program (Biosystems). The ratios of integrated intensities of MTCBP-1 to β-actin are displayed in figure 6. There was an increased expression (~2-fold, $\rho = 0.044$) of endogenous MTCBP-1 protein in HepG2 cells that were lipid overloaded when compared with MTCBP-1 expression from control HepG2 cells grown in medium containing BSA. A 1.6-fold increased expression of MTCBP-1 ($\rho = 0.026$) was evident in lipid overloaded HepG2 cells compared with MTCBP-1 expression in HepG2 cells grown in normal culture medium. Levels of β-actin were found to be minimally affected by free fatty acid overloading in HepG2 cells.

The HepG2 fat cell model was used to investigate the relationship between steatosis and MTCBP-1 expression. Linoleic acid was chosen in this study because of its known ability to be converted into arachadonic acid, a potent modulator of inflammation [18]. An increase in the triglyceride levels was found in the HepG2 cells that had been exposed to fatty acids conjugated to BSA. In addition the western blot analyses revealed that the expression of

endogenous MTCBP-1 was increased in HepG2 lysates that had been incubated with medium containing fatty acids. This was further verified by the increased integrated intensity ratio of MTCBP-1 to β-actin in blots from lysates of HepG2 cells incubated with LA-BSA. Hepatic steatosis results if the levels of triglycerides formed from large amounts of fatty acids exceed the capacity of the liver to form and secrete very-low-density lipoproteins (VLDL) [30]. This can occur when there is a defect in the mechanisms that involve mitochondrial fatty acid β-oxidation, peroxisomal oxidation and apolipoprotein formation [32]. Based on the liver cell data, the increased expression of MTCBP-1 during triglyceride accumulation may suggest a relationship between the protein and triglyceride synthesis. Therefore, it is of future interest to determine whether MTCBP-1 is involved with apoproteins which are known to provide a transport system for lipids.

3.4 Triglyceride overloaded and transfected HepG2 cells do not affect MTCBP-1 overexpression

HepG2 cells grown in medium containing fatty acids were transfected with plasmids encoding *N*-terminal c-myc tagged MTCBP-1 to determine whether cellular triglycerides affect the expression pattern of expressed MTCBP-1 (Figure 7). Control experiments which included HepG2 cultures grown in a medium containing either BSA or normal culture growth medium were set up to determine if BSA may also affect MTCBP-1 expression. There was no difference in the amount of expressed MTCBP-1 from HepG2 cells incubated with fatty acids compared with controls in all three experiments (Figure 8).

Another intriguing finding is that HepG2 transfections with plasmid encoding MTCBP-1 have reduced lipid accumulation. From the western blots, the signal intensities of overexpressed MTCBP-1 is similar to that of control experiments. This reduction in lipid accumulation when MTCBP-1 is overexpressed suggests a protective role of this molecule in NAFLD. We hypothesise a mechanism by which MTCBP-1 may influence lipid metabolism. Firstly, synthesis of triglycerides from exogenous polyunsaturated results in the induction of MTCBP-1 in the cell. However, when there is overexpression of this molecule, the cell may compensate by switching off the TG synthesis to allow for more fatty acid oxidation by induction of transcription factors, hence the reduction in lipid synthesis.

3.5 Subcellular localisation of MTCBP-1 in HepG2 cells

Immunofluorescence analysis was used to examine the subcellular localisation of MTCBP-1 in transfected and untransfected HepG2 cells that were subjected to lipid overloading. The two controls (BSA-treated cells and untreated HepG2 cells) were also analysed to determine any noticeable differences in MTCBP-1 physiology. The cells that were transfected with tagged MTCBP-1 construct were analysed for double immunofluorescence using peptide purified anti-rabbit polyclonals against MTCBP-1 and monoclonal anti-cmyc antibody (Figure 8). The endogenous MTCBP-1 was detected using anti-rabbit antibody against MTCBP-1 (Figure 9). The results on double probing with anti-MTCBP-1 antibody and anti-cmyc monoclonal antibody indicate that MTCBP-1 is expressed in the cytoplasm and nucleus of the cell. The transfected HepG2 cells that were grown in LA-BSA displayed a porous cytoplasm which is indicative of cytoplasmic lipid droplets. No significant differences were seen in the amount of protein distribution from lipid overloaded HepG2; BSA-treated HepG2 and untreated HepG2 cells. The photographs of transfected HepG2 demonstrate that MTCBP-1 is equally distributed in the nucleus and the cytoplasm. By contrast, c-myc protein was found to be primarily localised in the cytoplasm, with very weak fluorescence seen in the nucleus. The endogenous MTCBP-1 was also found to be localised in the cytoplasm and nucleus with no differences observed in the amount of protein distribution between the two compartments. Thus, the expressed protein is located in the same subcellular compartments as the endogenous MTCBP-1, deducing that expression into HepG2 does not alter MTCBP-1 distribution or its physiology.

Immunostaining of endogenous MTCBP-1 in HepG2 cells indicated that the protein was located in the nuclear compartment. The same was found in cells transfected with pSG5 plasmid encoding c-myc-MTCBP-1. In contrast, when the monoclonal c-myc antibody was used to probe the fusion protein, the distribution of the protein was primarily to the cytoplasm, with very weak nuclear fluorescence. This may suggest that the N-terminal c-myc tag had interfered with the nuclear localisation signal of MTCBP-1. The nuclear localisation signals are short stretches of positively charged amino acids (containing amino acids such lysine) that mediate the transport of nuclear protein to the nucleus *via* recognition by nuclear transport receptors [31].

4 Conclusion

Steatosis may be a result of impaired fatty acid utilisation in the hepatocyte or an increase in fatty acid intake or biosynthesis. Large amounts of triglycerides in the liver can elevate the generation of free radicals and lipid peroxidation that predispose the hepatocyte to injury [19]. In conclusion, from our observations, HepG2 human hepatoma cells are a useful model to study polyunsaturetd fatty acid metabolism under suitable experimental conditions. We have shown the accumulation of cellular triglycerides when the cells are grown in FA-rich

medium under a suitable experimental conditions. The cellular triglycerides increased the endogenous expression of MTCBP-1 in HepG2 cells overloaded with FFA; however, the molecular mechanism through which triglycerides alter the concentration of MTCBP-1 is yet to be determined.

Acknowledgments
Professor Motoharu Seiki for his donation of the MTCBP-1 cDNA,
Professor Grant Ramm, QIMR, for donation of the HepG2 strain.

Abbreviations
NAFLD- Non-alcoholic fatty liver disease
NASH- Non-alcoholic steatohepatitis
MTCBP-1- Metalloproteinase cytoplasmic-tail binding protein-1
VLDL- very low density lipoproteins
LA-BSA- Linoleic acid conjugated bovine serum albumin

Figures for manuscript

Fig. 1: Alignments of amino acid sequences of human MTCBP-1 and its homologues (human Sip-L, K oxytoca, S cerevisae, B. subtilis, Oryza sativa and mouse). I dentical residues are: red with yellow background in all 7 sequences or ii) blue with light blue background for 2 or moresequences. The conserved β-barrel fold of the ARD proteins overlined. Consensus indicates all matching residues. The alignment was performed using Vector NTI suite from sequences deposited from NCBI.

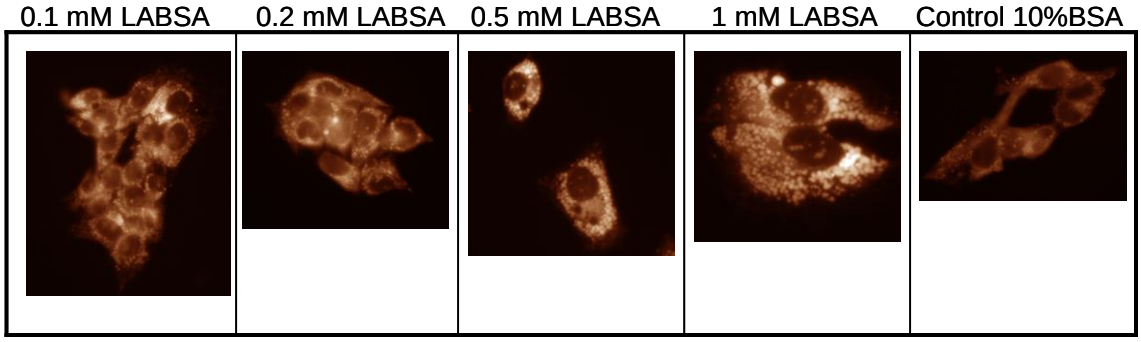

Fig. 2: Nile red fluorescence of lipid overloaded HepG2 cells. The cells were treated for 24 hr with varying concentrations of LABSA (A-D) constituting 0.1mM; 0.2mM 0.5mM and 1 mM. The cells were fixed with 4% paraformaldehyde prior to staining with 100ug/mL nile red dye. Cells were viewed under a fluorescent microscope at X40 magnification

Fig. 3: PCR amplification of three selected clones of C-myc tagged *MTCBP-1* construct. 1µg of pSG5-*MTCBP-1* containing the 5' UTR and coding sequence was used as a template for the PCR in a 50 µl total reaction volume. *MTCBP-1* specific primer pair was added to the reaction mix at 1µM final concentration. A PCR amplicon of 576 bp, typical of the tagged *MTCBP-1* was obtained. Two secondary products which represent the supercoiled (~4.7 kB) and nicked (3 kB) pSG5-MTCBP-1 plasmid could also be seen.

	Treatment 0.5 mM LA-BSA Average TG/P	Controls		FFA/BSA		FFA/Normal		P value
		10% BSA Average TG/P	Normal medium Average TG/P					
HepG2 cells	0.592	0.328	0.066	↑	1.8	↑	8.9	0.001
Transfected HepG2	0.155	0.112	0.111	↑	1.4	↑	1.4	0.067
Control HepG2 (Lipofectamine)	0.069	0.068	0.057	↑	1.0	↑	1.2	0.577

Table 1: Tabulation of cellular triglycerides analysed from treatment of HepG2 cells, transfected HepG2 cells and lipofectamine reagent (no DNA) transfected HepG2 cells. HepG2 cells were grown in media containing 0.5 mM LA-BSA. 10% BSA (control) or normal culture medium (control). The averages of triglyceride to protein ratio (TG/P) were calculated in all experiments. The ratios (fold-changes) of triglycerides analysed from FFA and controls are displayed and the arrow represents an up-regulated expression of triglycerides in FFA treated cells. A One Way Anova was used for statistical analysis between the treated and control HepG2 cells.

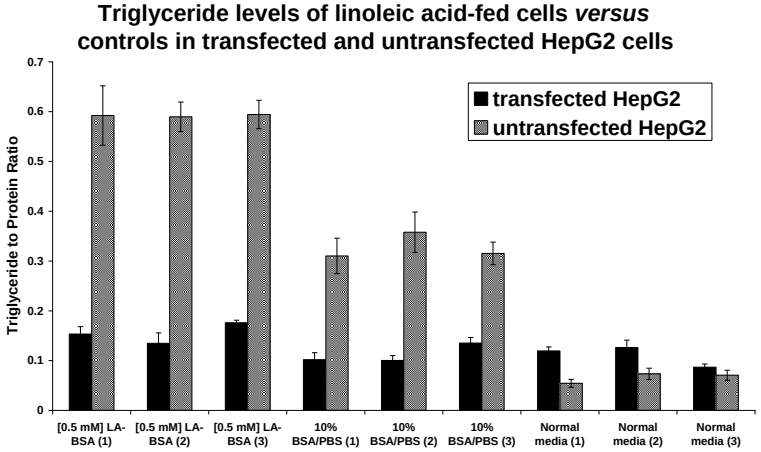

Fig. 4: Triglyceride levels of LABSA (A) and OABSA (B) fed HepG2 cells. The experiment was set up in triplicates in six well tissue culture plates. Two controls were included which consisted of the BSA treated cells and untreated HepG2 cells.

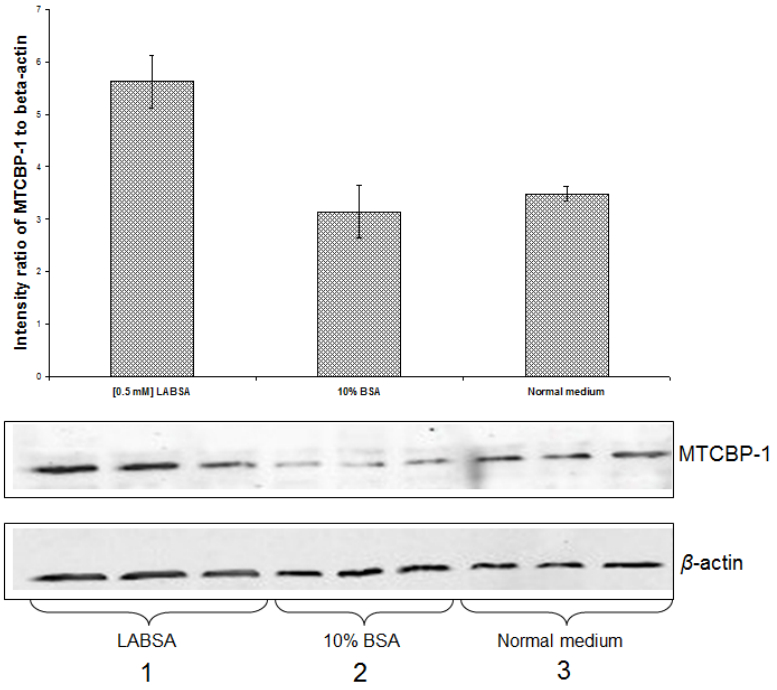

Fig. 5: Integrated intensities from western blots for quantitation of MTCBP-1 from cell lysate of LA-BSA overloaded HepG2 cells and HepG2 control cells grown in medium containing either BSA or normal culture medium. 10µg of proteins were loaded per well in triplicates. The blots were probed with anti-rabbit anti-MTCBP-1 and anti-mouse anti-β-actin. Immunoflourescence secondary antibodies Alexa 680 and Alexa 800 were used to view the blots using the Odyssey fluorescent scanner. The intensities from western blots were derived from the Odyssey scanner. Mean ± SE were: 5.6±0.50; 1.7±0.09; 3.91±0.30 for [0.5mM] LA-BSA, 10% BSA and normal media, respectively.

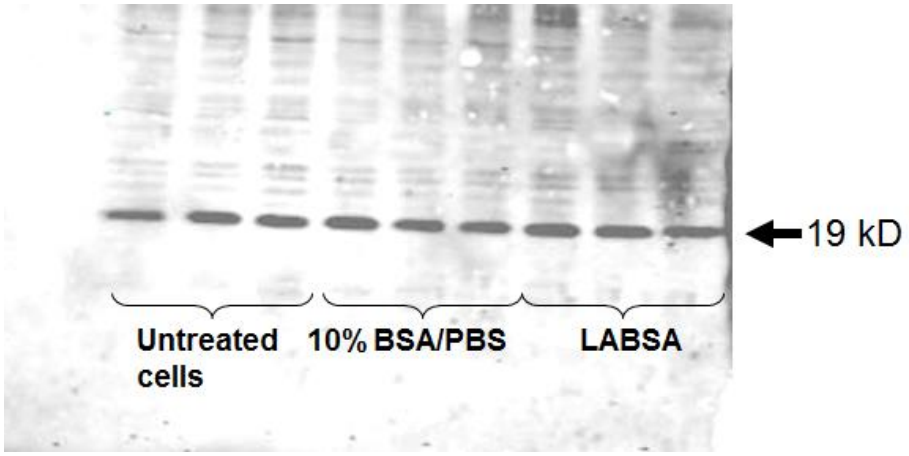

Fig. 6: Western blots analysis of overexpressed MTCBP-1 from HepG2 cells that were overloaded with lipids prior to transfections. HepG2 cells were grown in triplicate in medium containing 0.5 mM LA-BSA. Control experiments consisting of HepG2 cells grown in a medium containing either 10% BSA or normal culture growth medium were also analysed. HepG2 cells were incubated with fatty acids for 24 h prior to transfections with plasmids encoding c-myc MTCBP-1 A 20 µg of the reduced protein was loaded per well and separated on 14% SDS-PAGE gel for 1.5 h at 150V constant voltage. The proteins were transferred to the nitrocellulose membrane and blocked for 1h in 3% (w/v) fish gelatine in PBS. The proteins were probed with the anti-cmyc monoclonal antibody (Sigma) (1: 2000 dilution) A fluorescent secondary antibody (A680) prepared in 1:10 000 dilutions in blocking buffer was used to view the blots using the Odyssey scanner.

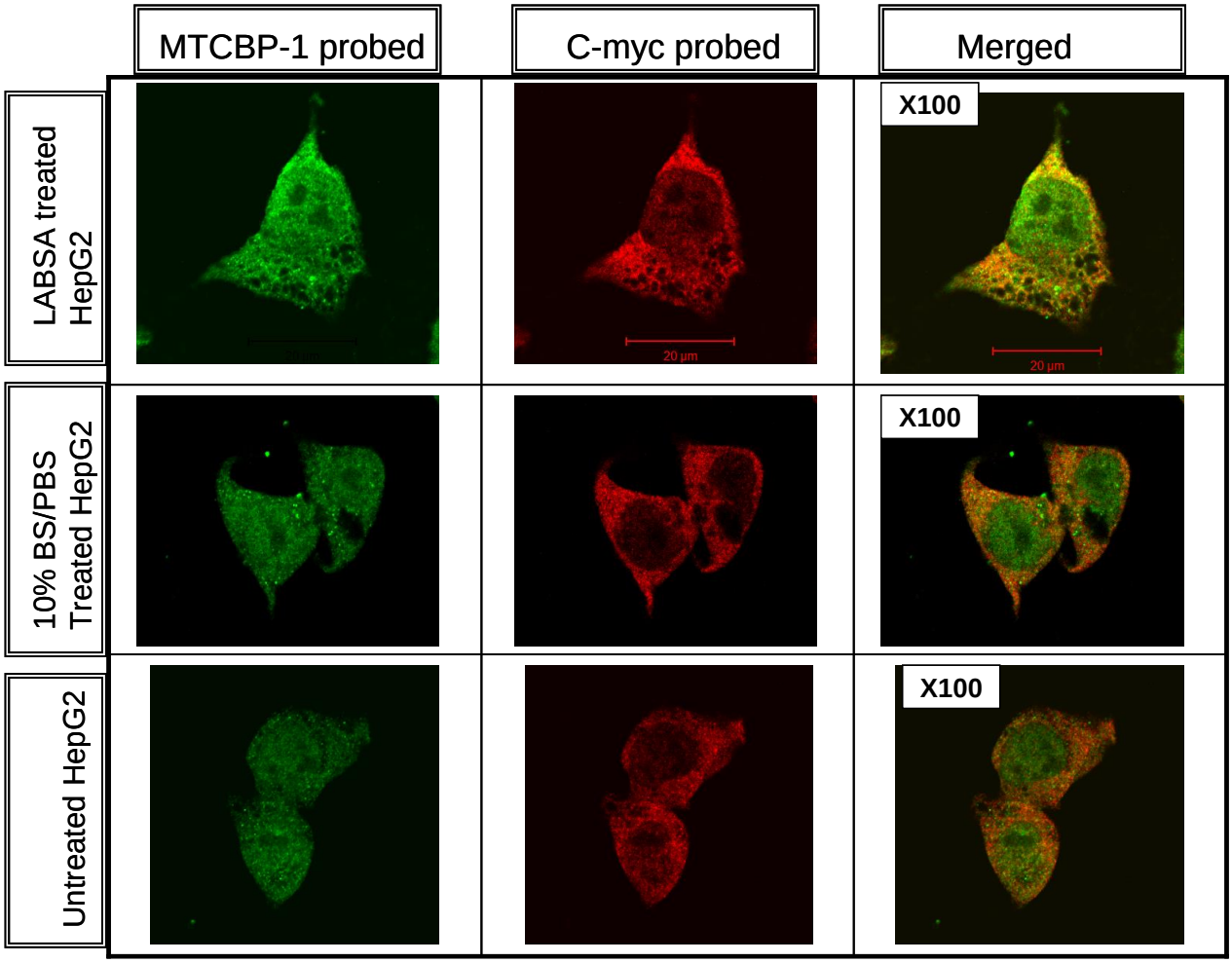

Fig. 7: HepG2 cells grown on coverslips were transfected with expression plasmid for c-myc and MTCBP-1 detection. After fixation in 4% paraformaldehyde, the cells were incubated with monoclonal anti-c-myc antibody and polyclonal anti-MTCBP-1 antibodies for 2 hours and overnight respectively. The bound antibodies were visualised with Alexa594-conjugated anti-mouse IgG (red) and Alexa488-conjugated anti-rabbit IgG (green). The fluorescence was analysed using a confocal microscope.

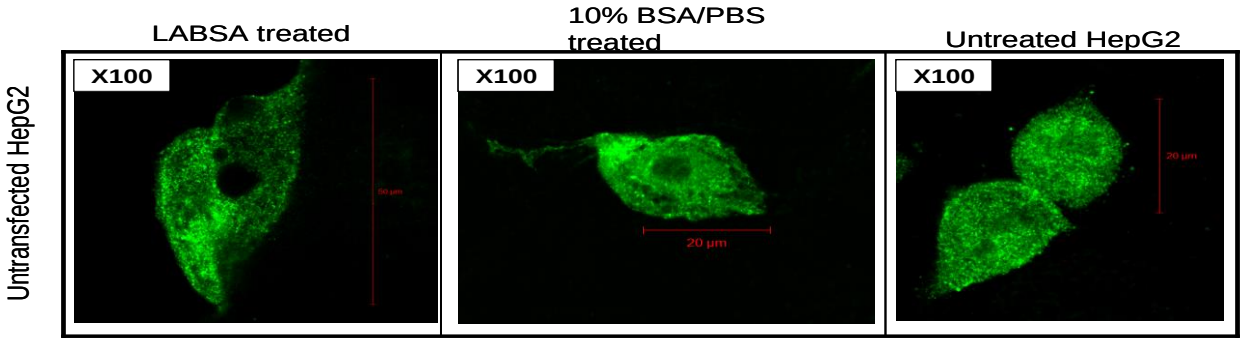

Fig. 8: Localisation of endogenous MTCBP-1 was analysed by immunoflourescence using antibodies against MTCBP-1. Following fixation, the cells were treated with anti-rabbit anti-MTCBP-1 antibodies for detection of the protein. For visualisation, Alexa488-conjugated anti-rabbit IgG (green) were used. Confocal microscopy was used to analyse the cells fluorescence.

References

1. Cortez-Pinto, H., Carneiro De Moura, M., Day, C.P. (2006) Non-Alcoholic Steatohepatitis: From Cell Biology to Clinical Practice. *Journal of Hepatology* **44**, 197-208.
2. Nehra, V., Angulo, P., Buchman, A., Lindor, K. (2001) Nutritional and Metabolic Considerations in the Etiology of Non-Alcoholic Steatohepatitis. *Digestive Diseases and Sciences* **46**, 2347-2352.
3. Letteron, P., Fromenty, B., Terris, B., C.Degott, Pessayre, D. (1996) Acute and Chronic Hepatic Steatosis Lead to in Vivo Lipid Peroxidation in Mice. *Journal of Hepatology* **24**, 200-208.
4. Tang, D., La, E., Kern, J., Kehrer, J. (2002) Fa Oxidation and Signaling in Apoptosis. *Journal of Biological Chemistry* **383**, 425-442.
5. Hirano, W., Gotoh, I., Uekita, T., Seiki, M. (2005) Membrane-Type 1 Metalloproteinase Cytoplasmic Tail Binding Protein-1 (Mtcbp-1) Acts as an Eukaryotic Aci-Reductone Dioxygenase (Ard) in Methionine Salvage Pathway. *Genes to Cells* **10**, 565-574.
6. Egebald, M., Werb, Z. (2002) New Functions for the Matrix Metalloproteinases in Cancer Progression. *Nature Reviews Cancer* **2**, 161-166.
7. Uekita, T., Gotoh, I., Kinoshita, T., Itoh, Y., Sato, H., Shiomi, T., Okada, Y., Seiki, M. (2004) Membrane-Type 1 Matrix Metalloproteinase Cytoplasmic Tail-Binding Protein-1 Is a New Member of the Cupin Family. *Journal of Biological Chemistry* **279**, 12734-12743.
8. Seiki, M. (2002) The Cell Surface: The Stage for Matrix Metalloproteinase Regulation and Migration. *Current Opinion in Cell Biology* **14**, 624-632.
9. Itoh, Y., Takamura, A., Ito, N., Maru, Y., Sato, H., Suenaga, N., Aoki, T., Seiki, M. (2001) Homophilic Complex Formation of Mt1-Mmp Facilitates Prommp-2 Activation on the Cell Surface and Promotes Tumor Cell Invasion. *EMBO Journal* **20**, 4782-4793.
10. Dunwell, J.M., Culham, A., Carter, C.E., Sosa-Aguirre, C.R., Goodenough, P.W. (2001) Evolution of Functional Diversity in Cupin Superfamily. *Trends in Biochemical Sciences* **26**, 740-746.
11. Yeh, C.-T., Lai, H.-Y., Chen, T.-C., Chu, C.-M., Liaw, Y.-F. (2001) Identification of a Hepatic Factor Capable of Supporting Hepatitis C Virus Replication in a Nonpermissive Cell Line. *Journal of Virology* **75**, 11017-11024.
12. Machado M.V., Cortez-Pinto H. (2013) Non-invasive diagnosis of non-alcoholic fatty liver disease-A critical appraisal. *Journal of Hepatology* **58** 1007–1019
13. Takahashi Y., Soejima Y., Fukusato T. (2012) *World J Gastroenterology* **18** (19): 2300-2308
14. Leamy A.K., Egnatchik R.A, Young J.D. (2013) Molecular mechanisms and the role of saturated fatty acids in the progression of non-alcoholic fatty liver disease *Progress in lipid research* **52** 165–174
15. Matteoni C., Younossi Z., Gramlich T. (1999) Non Alcoholic Fatty Liver Disease: A spectrum of Clinical and Pathological Severity. *Gastroenterology* **116** 1413-1419
16. Angulo P. (2002) Medical Progress: Non Alcoholic Fatty Liver Disease. New England Journal of Medicine 346 1221-1231
17 Adams L.A., Talwalkar J.A. (2006) Diagnostic evaluation of Nonalcoholic fatty liver disease. *Journal of Clinical Gastroenterology* **40** S34-S38
18. Janorkar A.V., King K.R., Megeed Z., Yarmush M.L. (2009) Development of an In Vitro Cell Culture Model of Hepatic Steatosis Using Hepatocyte-Derived Reporter Cells. *Biotechnology and Bioengineering* **102** (5) 2009
19. Brent A., Neuschwander-Tetri B., Caldwell S. (2003) Non-Alcoholic Steatohepatitis: Summary of AASLD Single Topic Conference. *Hepatology* **37**, 1202-1219
20. Leonard D., Michael K., Peter C., Selden C., Humphrey H. (2007) Fat-loaded HepG2 Spheroids Exhibit Enhanced Protection from Pro-Oxidant and Cytokine Induced Damage. Journal of Cellular Biochemistry **101** 723-734
21. Marra C. (1992) Incorporation and Metabolic Conversion of Unsaturated Fatty Acids in SK-Hep1 Human Hepatoma Cells in Culture. *Molecular and Cellular Biochemistry* **117** 107-118
22. Xujun W., Hongshi J., Henry G.N. (1996) Low rate of ApoB secretion from HepG2 Cells Result in Reduced Delivery of Newly Synthesised Triglycerides to a "Secretion-Coupled" Pool. *Journal of Lipid Research* **37** 1198-1206
23. Mason T., (1998) The Role of Factors that Regulate the Synthesis and Secretion of Very-Low-Density-Lipoproteins by Hepatocytes. *Critical Reviews in Clinical Laboratory Sciences* **35** 461-487
24. Pagano G., Pacini G., Musso G., Gambino R., Mecca F., Depetris N, *et al.* (2002) Non-alcoholic steatohepatisis, insulin resistance and metabolic syndrome: further evidence of an etiological association. *Hepatology* **35** 367-372
25. Day C.P., James O.F. (1998) Steatohepatitis: A tale of two "hit"? *Gastroenterology* **114** 842-845
26. Damelin L.H., Kirwan M., Collins P., Selden C., Humphrey J.F. (2007) Fat-loaded HepG2 Spheroids Exhibit Enhanced Protection from Pro-oxidant and Cytokine-Induced Damage. *Journal of Cellular Chemistry* **101** 723-734.
27. Marra C. (1992) Incorporation of Metabolic Conversion of Unsaturated Fatty Acids in SK-Hep1 Human Hepatoma Cells in Culture. Molecualr and Cellular Biochemistry **117** 107-118.
28. Wu Xujun S.A., Jiang H., Ginsberg H.N. (1996) Low Rates of ApoB secretion from HepG2 Cells Result from Reduced Delivery of Newly Synthesised Triglycerides to a 'Secreted-Coupled' Pool. *Journal of Lipid Research* **37** 1198-1206.
29. Sanyal A.J. (2005). The pathogenesis of NASH: Human Studies. *Fatty Liver Disease: NASH and related disorders*. 76-90.
30. Mason T. (1998). The Role of Factors That Regulate the Synthesis and Secretion of Very-Low-Density -Lipoprotein by Hepatocytes. *Critical Reviews in Clinical Laboratory Sciences* **35** 461-487.
31. Xiao Z., Liu X., Henis Y.I., Lodish H.F. (2000) A Distinct Nuclear Localisation Signal in the N-terminus of Smad 3 Determines its Ligand Induced Nuclear Translocation. *PNAS* **97** 7853-7858.
32. Okamoto Y., Tanaka S., Haga Y. (2002) Enhanced Glut2 Gene Expression in an Oleic Acid-Induced in-vitro fatty liver model. *Hepatology Research* **23** 138-144
33. Kent S.B. (1988) Chemical Synthesis of Peptides and Proteins. *Annual Reviews in Biochemistry* **57** 957-989
34. Suzuki A., Lindor K., St Saver J., Lymp J., Mendes F., Muto A., Okada T., Angulo P. (2005) Effect of changes on body weight and lifestyle in nonalcoholic fatty liver disease. Journal of Hepatology 43 1060–1066

www

Appendix A

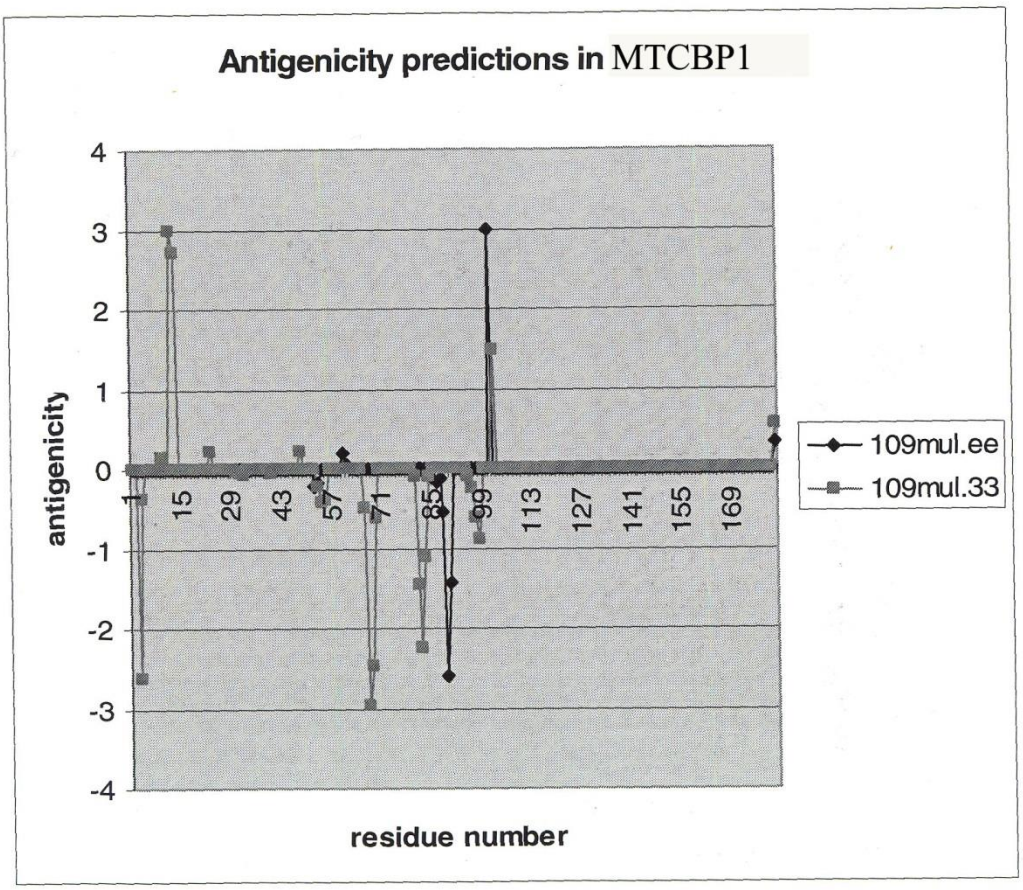

179 aa

MVLAWYMDDAPGDPRQPHRPDPGRPVGLEQLRRLGVLYWKLDADKYENDP 50
ELEKIRRERNYSWMDIITICKDKLPNYEEKIKMFYEEHLHLDDEIRYILD 100
GSGYFDVRDKEDQWIRIFMEKGDMVTLPAGIYHRFTVDEKNYTKAMRLFV 150
GEPVWTAYNRPADHFEARGQYVKFLAQTA 179

A1: Preditop Predictions for antigenicity: The amino acid sequence of MTCBP-1 was analysed using Preditop Algorithm for antigenic peptide epitoped. The turn scales –mul.ee and –mul.33 correspond to helical and hairpin turns (as displayed by sharp peks) and these are regions of exposed turns and loops, where hydrophilic peptides are commonly found. The highlighted peptide sequence represents the antigenic regions. Peptide 1 (P1): **DAPGDPRQPHR**; Peptide 2 (P2): **DGSGYFDVRDK.**

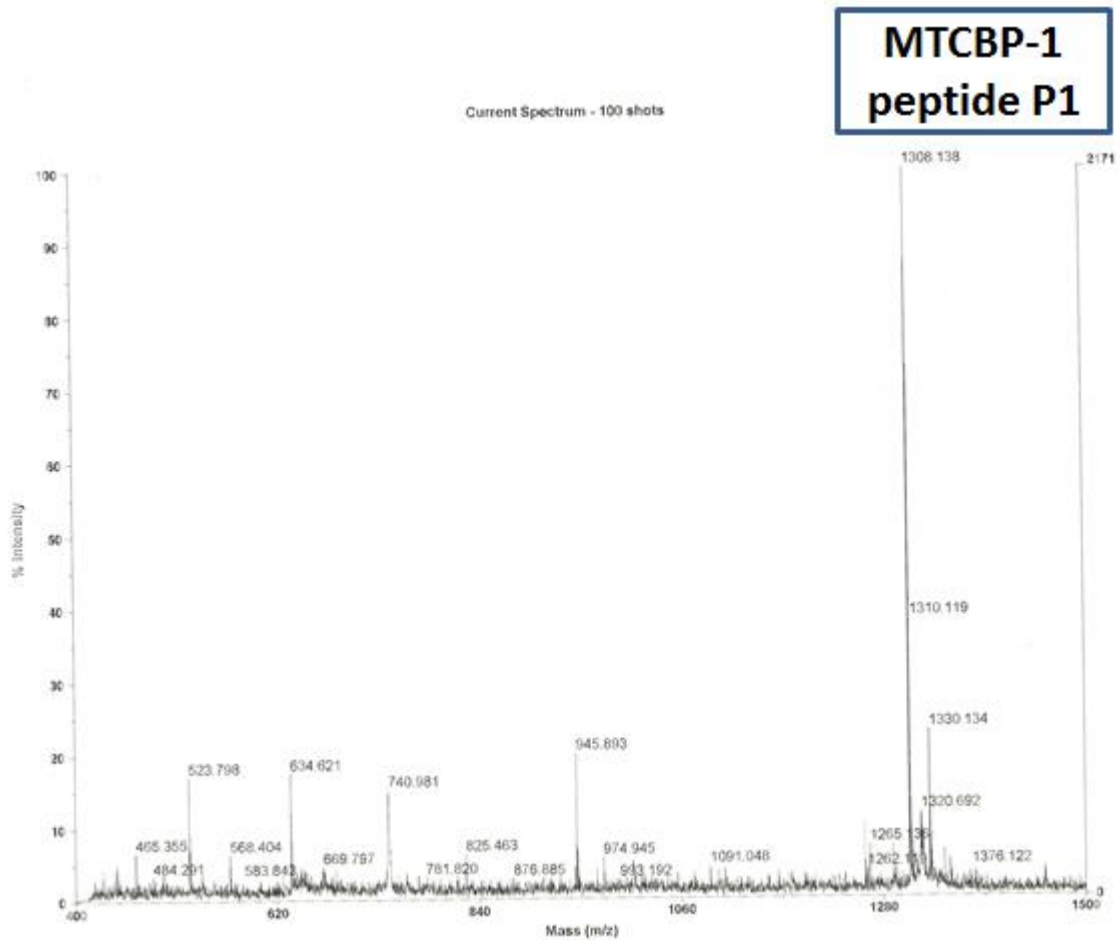

A2: Mass Analysis of HPLC-purified P1 peptide of MTCBP-1 protein by MALDI-TOF mass spectrometry. The peptide at a ratio of 1:2 to the MALDI-TOF matrix was added onto a mass spectrometry plate, in duplicates. The plate was air-dried before mass analysis by MALDI-TOF. The highest peak at 1308.138 was consistent with the calculated molecular weight of P1 peptide (1308 Da).

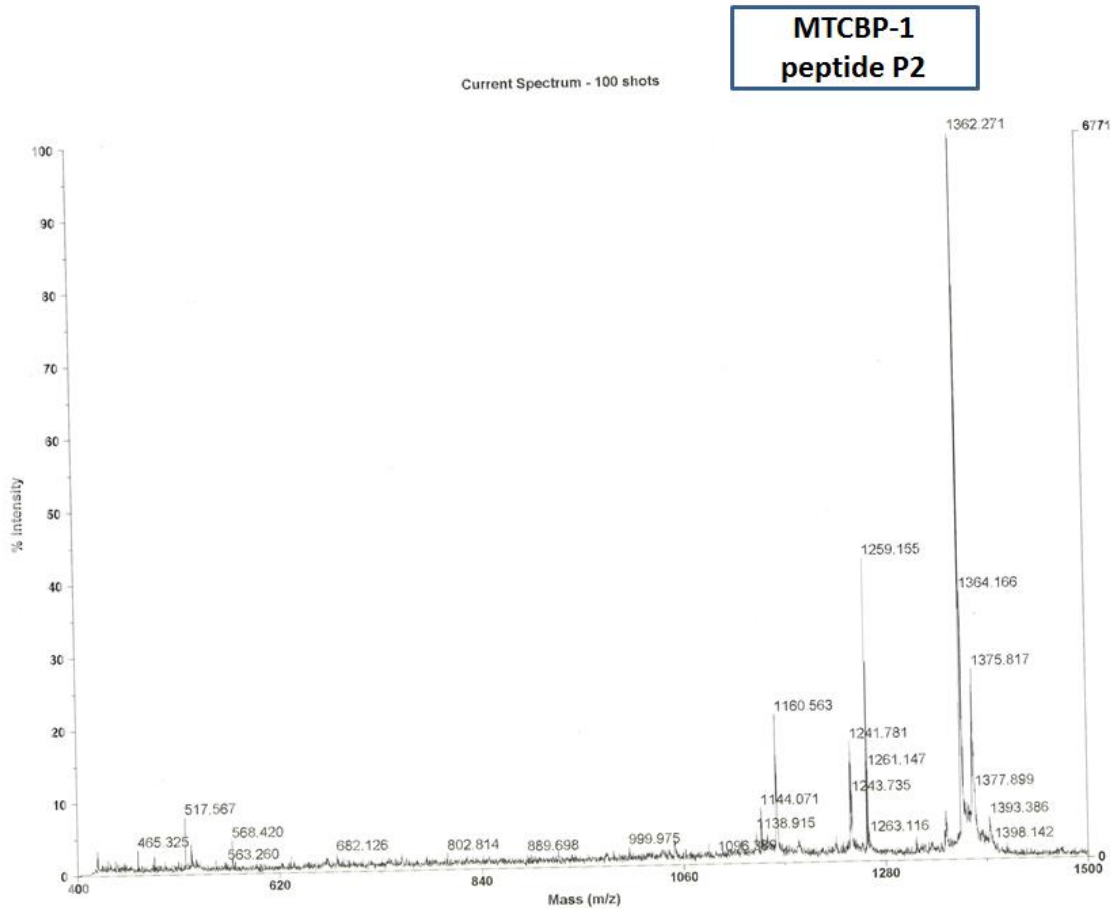

A3: Mass Analysis of HPLC-purified P2 peptide of MTCBP-1 protein by MALDI-TOF mass spectrometry. The peptide at a ratio of 1:2 to the MALDI-TOF matrix was added onto a mass spectrometry plate, in duplicates. The plate was air-dried before mass analysis by MALDI-TOF. The highest peak at 1362.271 was consistent with the calculated molecular weight of P2 peptide (1362 Da).

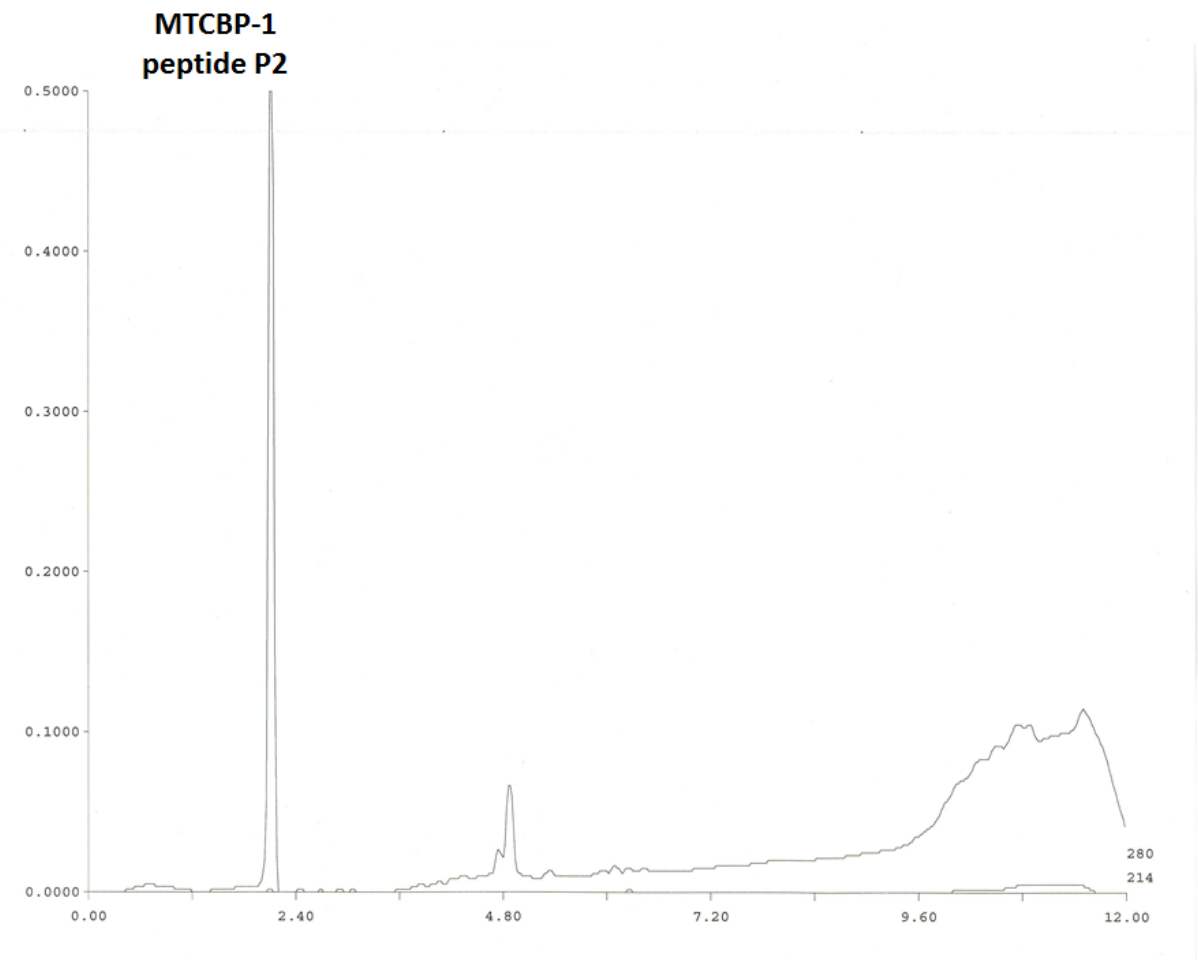

A4: The elution profile of P1 peptide epitope of MTCBP-1 protein. Analysis of the peptide purity and retention time was performed by RP-HPLC at wavelengths of 230-240 nm. The major peak eluted at 2.35 minutes corresponds to the P1 peptide. The fraction was collected and peptide mass was confirmed by MALDI-TOF mass spectrometry.

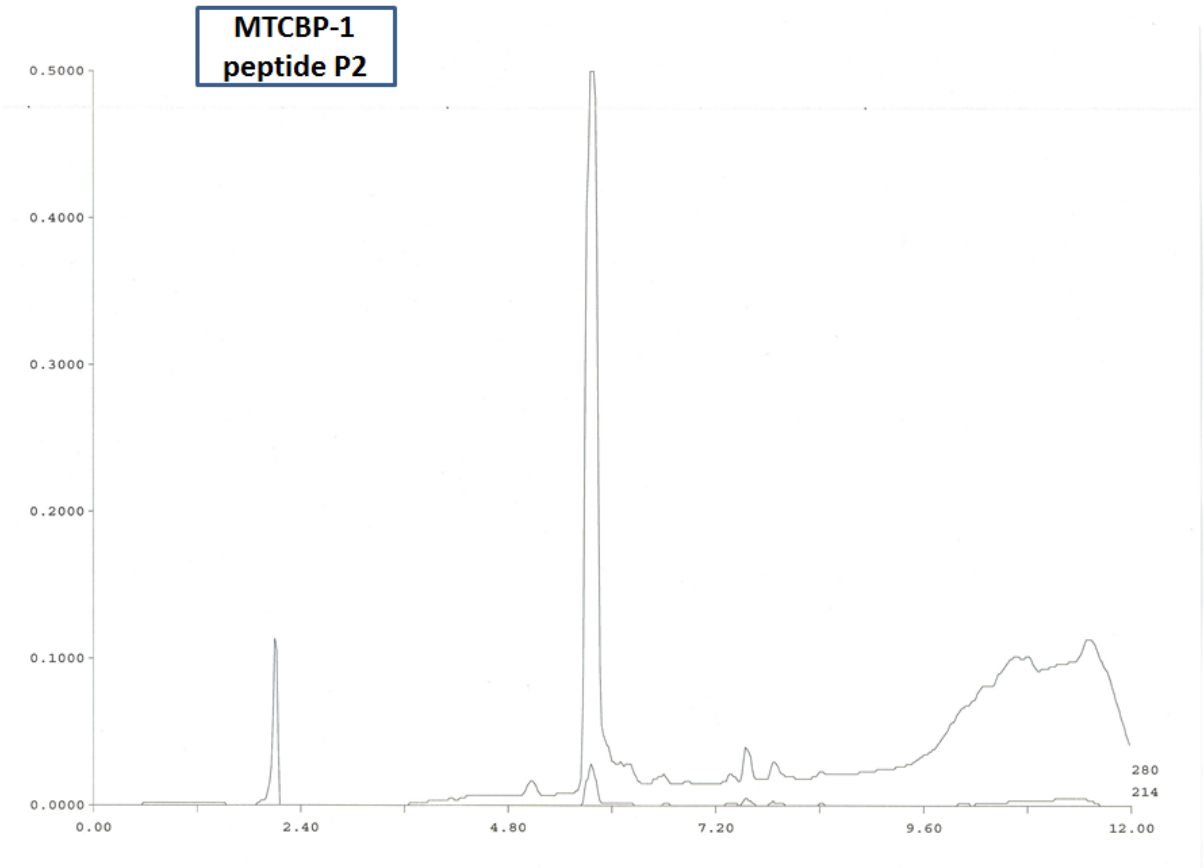

A5: The elution profile of P2 peptide epitope of MTCBP-1 protein. Analysis of the peptide purity and retention time was performed by RP-HPLC at wavelengths of 230-240 nm. The major peak eluted at 6 minutes corresponds to the P2 peptide. The fraction was collected and peptide mass was confirmed by MALDI-TOF mass spectrometry.

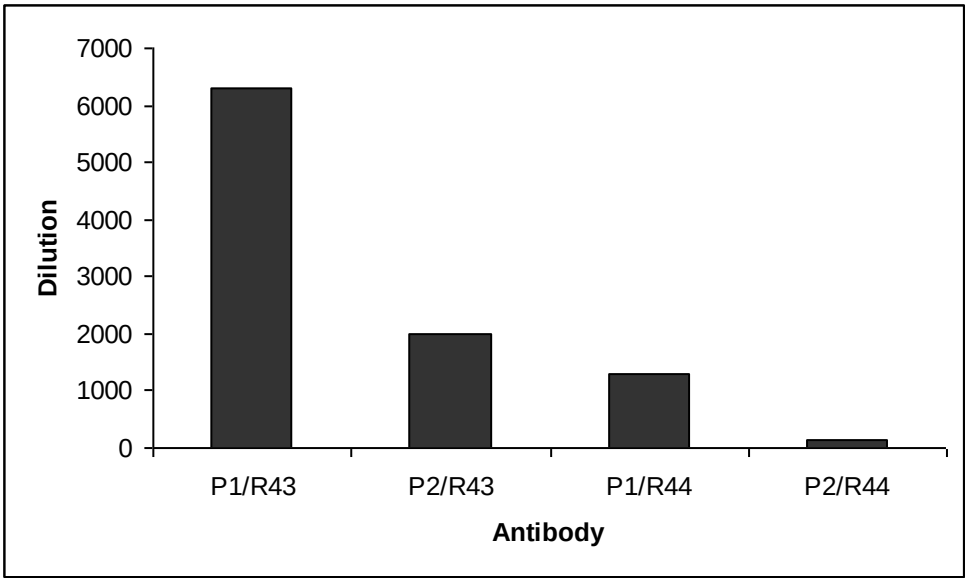

A6: ELISA measurements of anti-peptide antibody titres from serum obtained from rabbits 43 & 44. Rabbits were immunised with two peptide antigens (*P1* and *P2*). The sequences of the peptide antigens *P1* and, *P2* are *N*-LTSPSGPGYH and *N*-KKYQAIASNSK, respectively. The ELISA assay was performed in a 96-well microtitre plate. Peptides (2 µg) were attached to 5% (w/v) glutaraldehyde. A dilution series of 1:50, 1:100, 1:200 and 1:400 of antisera in 1% (w/v) BSA was added in triplicate to the antigen coated plate. This was then followed by incubation of the plate with goat anti-rabbit IgG, conjugated with horseradish peroxidise (1:3000 dilution). OPD (o-phenylenediamine dihydrochloride) was used as a chromogen in the indirect ELISA assay. Antibody titres were determined from the absorbances at $\lambda_{450\ nm}$ on a SpectraMax 250 (Molecular Devices).